A 3D microfluidic paper-based analytical device with smartphone-assisted colorimetric detection for iodine speciation in seaweed samples

Lorena Placer , Isela Lavilla, Francisco Pena-Pereira [*], Carlos Bendicho [*]

Centro de Investigación Mariña, Universidade de Vigo, Departamento de Química Analítica e alimentaria, Grupo QA2, Edificio CC Experimentais, Campus de Vigo, As Lagoas, Marcosende, 36310 Vigo, Spain

ABSTRACT

The present work reports on the development of a 3D origami microfluidic paper-based analytical device (3D μPAD) for the determination of iodide and iodate in edible seaweeds by smartphone-based colorimetric detection. In addition, a methacrylate holder was designed and fabricated to enhance interlayer contact in 3D μPADs, obtaining excellent sensitivity and precision, also allowing real-time monitoring in a straightforward and expeditious way. The reported assay, based on the formation of a blue colored triiodide-starch complex at the detection areas of the 3D μPAD, represents an affordable, fast and greener alternative for the simultaneous determination of inorganic iodine species. Under optimal conditions, the proposed method showed limits of detection and quantification of 9.8 and 32.7 μM for I^- and 0.6 and 1.8 μM for IO_3^-, respectively. The repeatability, expressed as relative standard deviation, was 1.7% and 3.3% for I^- and IO_3, respectively. The proposed 3D μPAD was applied to the determination of iodine species in extracts of edible seaweeds and related food additives, showing satisfactory recoveries (90–109%).

1. Introduction

Iodine is an essential micronutrient whose intake is commonly achieved by means of water and food products such as fish, shellfish, milk and iodine-fortified salt, among others. Furthermore, seaweeds have a biologic capacity to concentrate iodine from the seawater and are attracting a great deal of interest as alternative sources of dietary iodine, being considered as healthy and sustainable superfoods [1,2]. However, both excessive and deficient iodine intake can lead to altered thyroid function [3,4]. Thus, iodine deficiency disorders such as goiter, hypothyroidism, impaired mental function, spontaneous hyperthyroidism in the elderly, iodine-induced hyperthyroidism and increased susceptibility of the thyroid gland to nuclear radiation have been reported [5], whereas hyperthyroidism, hypothyroidism, goiter and thyroid autoimmunity have been attributed to excessive iodine intake [6]. The National Research Council of US recommends a daily intake of 150 μg of iodine for adults [7]. The iodine content of seaweeds or foods containing seaweeds is currently not regulated in the European Union. Notwithstanding this, France and Germany have recommended a maximum level of iodine in seaweed of 2000 and 20 μg/g, respectively [2], and the European Commission has recently adopted the recommendation of

monitoring iodine in seaweed species, halophytes and food additives based on seaweed [8]. The bioavailability and toxicity of iodine species present in seaweeds has been reported to be variable [9,10]. Thus, assessing the concentration levels of iodine species in seaweeds would be required to optimize the iodine intake of the population within an optimal range.

Analytical methods reported in the literature for iodine speciation in seaweeds commonly involve inductively coupled plasma-mass spectrometric detection hyphenated with a number of chromatographic and electrophoretic separation techniques [10–14]. These methods show excellent sensitivity and selectivity, even though extended analysis times are required, and the advanced instrumentation used is expensive and not amenable for portability. In addition, extensive dilution is often required prior to analysis due to the high concentration levels of iodine species present in certain seaweeds. Alternative approaches have also been recently reported, including flow-based methods with potentiometric [13], spectrophotometric [13] and fluorimetric detection [15]. The development of straightforward, rapid and cost-effective analytical strategies involving everyday IT communications devices [16] for the simultaneous determination of iodine species in seaweeds and food additives based on seaweed would be highly desirable.

In recent years, microfluidic paper-based analytical devices (µPADs) are receiving much interest in different fields due to their low-cost, low sample consumption, easy fabrication and use. While two dimensions (2D) µPADs are commonly used, 3D µPADs allow multiplexed analyses to be performed with improved homogeneity at the detection areas [17]. 3D µPADs have demonstrated applicability in environmental monitoring [18–20], biological analysis [21–23] and chemical sensing [24,25]. 3D µPADs can be used as origami devices by folding them into one piece and aligning their reservoirs. The use of adhesive tapes [26], staples [27], clips [25] or clamps [20,28] to ensure close contact between the layers has been reported in the literature. Digitization of 3D µPADs for data acquisition occasionally requires unfolding the device and, depending on the holder used, real time analysis is not always possible. Therefore, the development of a holder that allows the analysis to be carried out quickly and reproducibly, being able to introduce the sample easily and check, in real time, the appearance of the detection area without the need to remove the 3D µPAD from the holder for analysis would be highly convenient.

The aim of this work is the development of a straightforward, rapid and cost-effective assay for the simultaneous determination of inorganic iodine species in edible seaweed and food additives based on seaweed. For this purpose, a 3D origami µPAD system with smartphone-assisted colorimetric detection was developed. To the best of our knowledge, this work represents the first non-instrumental detection method for iodine speciation analysis in seaweed samples. Furthermore, a universal holder for 3D µPADs that ensured a reproducible cellulose substrate interlayer contact while facilitating digitization and data acquisition was fabricated and presented in this work.

2. Experimental

2.1. Reagents and materials

All reagents were of analytical reagent grade. High-purity deionized water was produced from a Millipore Sigma Simplicity ultrapure water system (Millipore Iberian S.A., Madrid, Spain). Stock standard solutions were prepared from potassium iodide (Fluka Chemie, Busch, Switzerland) and potassium iodate (Merck, Darmstadt, Germany). The following reagents were also used: starch, citric acid monohydrate, choline chloride (ChCl), glycerol, urea and sodium phosphate from Sigma-Aldrich (St. Louis, MO, USA); agarose from Ecogen (Barcelona, Spain); polyvinylpyrrolidone (PVP) from Fluka; oxalic acid, potassium bromide, sodium sulfate and magnesium chloride from Merck; glucose and sodium nitrite from Panreac (Barcelona, Spain); potassium chloride, sodium chloride and potassium nitrate from Prolabo (Paris, France); sodium hydrogen carbonate from Carlo Erba (Milan, Italy); potassium nitrate from Probus (Badalona, Spain) and humic acid from Fluka Chemie (Buchs, Switzerland).

2.2. Apparatus

A Xerox ColorQube 8580 printer (Rochester, New York, USA) and a Phoenix instrument RSM-02HP+ magnetic stirring hot plate (Garbsen, Germany) were used for defining hydrophobic barriers on Whatman No. 1 filter paper (Maidstone, Kent, UK) by wax printing technology. A Huawei P8 Lite 2017 smartphone (Huawei, Shenzhen, China) and a portable PULUZ photo studio lightbox (Shenzhen PULUZ Technology Limited, Shenzhen, China) equipped with 20 LEDs were used for smartphone-based colorimetric detection. The holder design was carried out by SolidWorks 2022 software (Dassault Systèmes-SolidWorks Corporation, Massachusetts, USA) and was machined using a DMG MORI CMX 70 U 5-axis milling machine (DMG MORI AKTIENGESELLSCHAFT, Bielefeld, Germany).

2.3. Data processing

The free image processing program ImageJ [29] was used for non-instrumental data acquisition. Alternatively, the App RGB Color Detector (The Programmer, Google Play Store) was used with this aim with the smartphone camera.

2.4. Design and fabrication of 3D µPADs

3D µPADs were pre-designed to create hydrophobic patterns by wax printing, thus defining the required hydrophilic reservoirs and fluidic channels. As shown in Fig. 1A, µPADs (60 mm × 19 mm) consisted on three independent squared zones, namely donor, reaction and detection areas (19 mm × 19 mm each one). The donor area (1) includes five circular reservoirs, the one at the middle (d=7 mm) used as the inlet for blanks, standards and/or seaweed sample extracts, and four reservoirs (d=4 mm) connected in a cross-shaped position with the central reservoir by 2.5 mm internal diameter channels. The reaction area (2) includes four separated circular reservoirs (d=4 mm) aligned with the four donor reservoirs mentioned above. Each reservoir of the reaction area can be modified with the required reagents to form a product (i.e. triiodide) that can subsequently react with the colorimetric reagent present in the detection area (3). The detection area (3) is composed of four separated circular reservoirs (d=3 mm) that can be modified with an appropriate colorimetric reagent for the determination of iodine species. Several µPADs were printed in a Whatman No. 1 filter paper and the wax pattern was heated at 100 °C for 2 min to embed the hydrophobic wax into the cellulose fiber matrix. Each µPAD was cut to use. The dimensions of the reservoirs and channels in each of the corresponding zones after fabrication of the µPADs are shown in Fig. 1B.

2.5. Design and fabrication of the methacrylate holder

A homemade methacrylate holder (35 mm × 35 mm) was designed to ensure a reproducible contact between the substrate layers of the 3D µPAD by enabling the aqueous solution to flow in the vertical direction. Schematic drawings and images of the single methacrylate holder and assembled with a 3D µPAD are shown in Fig. 2. The holder consists of two methacrylate squared pieces that fit together perfectly with a 1 mm ridge. Both pieces present a square hole (16 mm x 16 mm) in the center that facilitates both the sample introduction and real-time colorimetric
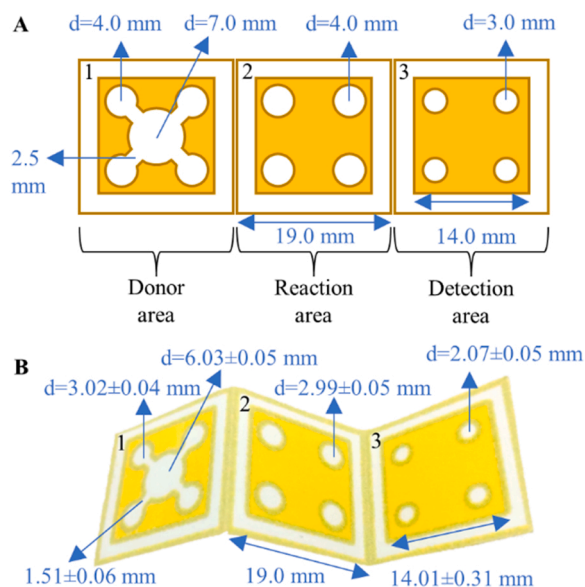

Fig. 1. Schematic design of 3D µPADs. Computer scheme of a 3D µPAD for iodine speciation analysis (A). Image of a printed and folded 3D µPAD (B).
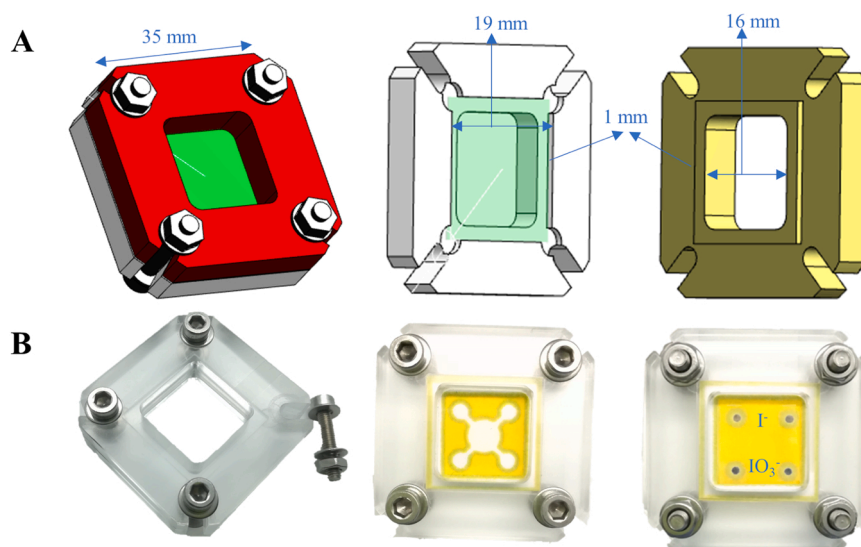
Fig. 2. Schematic illustration of the proposed methacrylate holder (35 mm × 35 mm). Scheme of computer design of the holder (A). Image of the methacrylate holder without and with the 3D μPADs, before and after analysis (B). The formation of colored products in the detection areas of the 3D μPAD enables the simultaneous determination of iodine species.

detection without the requirement to remove the PAD from the holder and unfolding it for analysis. The 3D μPAD remains firm and stable in the holder and ensures a sensitive and accurate analysis. In addition, the screw arrangement allows for quick and easy use.

2.6. Determination of iodide and iodate in seaweed extracts by the 3D μPAD with smartphone-based colorimetric detection

Both the reaction and detection areas of 3D μPADs prepared as described in *Section 2.4* were modified with chemicals before being applied to the determination of I^- and IO_3^- in seaweed samples. Thus, a volume of 5 μL of 100 mM citric acid was added to each of the four reaction areas to provide the required media for the iodometric reaction. In addition, 5 μL of 75 mM potassium iodide was added to two of the reaction zones for IO_3^- determination, whereas 5 μL of 75 mM potassium iodate was added to the remaining two reaction zones for I^- determination (*Fig. 1*). Finally, 10 μL of a 1% (m/v) starch solution was added in each detection area, and the 3D μPADs were dried in an oven for 30 min at 50 °C. For analysis, the 3D μPAD was placed into the methacrylate holder (*Section 2.5*) and 35 μL of a blank, standard or sample extract was added in the donor area of the 3D μPAD. Then, the holder was turned over and placed into a chamber with controlled luminosity for digitization of the detection areas of the 3D μPAD by a smartphone camera after 1 min (*Video S1*). The analytical response (i.e., mean color intensity difference in the green channel, ΔIc) of each detection area was obtained by processing the image using RGB Color Detector app or ImageJ software. A schematic of the experimental procedure for iodine speciation is shown in *Fig. S1*.

Supplementary material related to this article can be found online at doi:10.1016/j.snb.2022.133109.

Analysis of edible seaweed extracts by the above procedure required iodide and iodate extraction as described in the literature [9]. In brief, 1 g of ground seaweed was mixed with 5 mL of deionized water or 0.2 M HNO_3 and kept under stirring (1200 rpm) for 3 h. The mixture was then centrifuged for 10 min at 4000 rpm and filtrated. The filtrate was made to volume with ultrapure water and analysed using the above procedure.

3. Results and discussion

3.1. Optimization of experimental parameters

A 3D μPAD for the simultaneous colorimetric determination of iodine species was developed in this work. Experimental variables associated with the design of the μPAD, digitization and image processing conditions, as well as other parameters affecting the formation of a colored product in the detection areas of the μPAD, were optimized. The obtained results are provided in this section.

Firstly, a number of colorimetric reagents were assessed for the colorimetric sensing of the triiodide ion generated from both iodide and iodate in the reaction areas of the 3D μPAD. The formation of colored complexes with starch [30], agarose [31], and polyvinylpyrrolidone (PVP) [32–34] has been exploited in a number of colorimetric methods for determination of iodine species. In addition, several deep eutectic solvents (DESs) have been reported to form colored solutions upon uptake of iodine [35] and could be potentially applicable for sensing purposes. Accordingly, the effect of starch, agarose, PVP and four different DESs, namely ChCl-urea (1:2), ChCl-oxalic acid (1:1), ChCl-glucose (1:1) and ChCl-glycerol (1:2), on the analytical response has been evaluated. The analytical responses achieved with the different colorimetric reagents in RGB and grayscale (GS) modes are shown in Fig. 3. A careful selection of a specific RGB channel can help in attaining high sensitivity and selectivity for iodide and iodate determination. As can be deduced from the Figure, starch yielded the highest analytical response for both I^- and IO_3^-, especially when the green (G) channel was selected, on the basis of the well-known reaction between starch and the triiodide ion that leads to the formation of aggregates and loose fibrous networks forming a superhelix structure [36]. Remarkably, both red (R) and blue (B) channels were sensitive to the presence of iodine species, thus being eligible as alternative channels for quantitative analysis in particular applications where the G channel is ineffective. On the other hand, while GS yielded acceptable sensitivity, its selection was not considered for enhanced selectivity. The rest of colorimetric reagents assessed led to significant analytical responses in the presence of both iodine species, even though 1.5–16.2-fold lower than achieved with starch. Besides, mixtures of starch and agarose (1:1) or PVP (1:1) were studied, although the analytical response was slightly lower than the one obtained with starch (1.4–2.4-fold). Based on the above, starch was selected as the colorimetric reagent of choice, whereas the G color
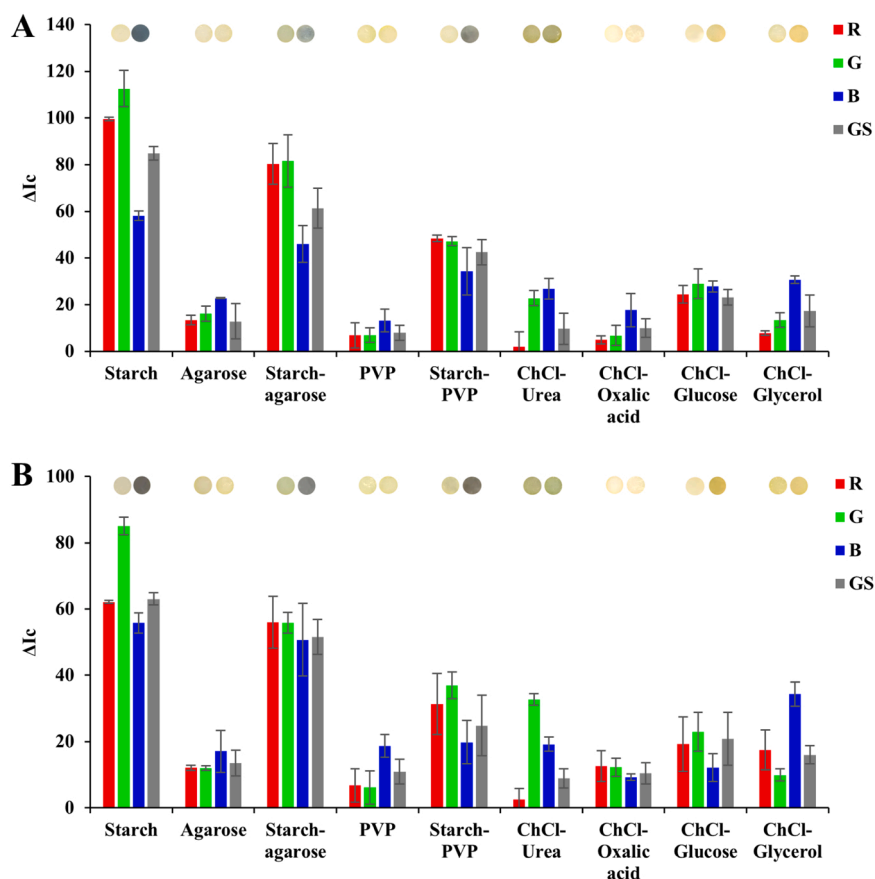
Fig. 3. Effect of the colorimetric reagents and color mode detection on the analytical signal (ΔI_c) for iodide (A) and iodate (B). The insets show the detection areas modified with each colorimetric reagent in the absence (left, blank) and presence (right, standard solutions) of iodine species.

channel was selected to attain the highest sensitivity.

The digitization conditions were then evaluated to achieve the highest sensitivity. This study included two adjustable parameters on the smartphone that allowed for greater control over the images, namely ISO and exposure value (EV). ISO is referred to the sensitivity of the sensor to capture light, whereas EV relates exposure time and camera lens aperture. As can be deduced from Fig. 4, the analytical response depended to a high extent on the EV value, showing the highest sensitivity at a + 1.0 level, while a minimal effect on the analytical response was observed by modifying the ISO values. So, the optimal conditions were 800 and + 1.0 for ISO and EV, respectively.

The analytical performance of five cellulose substrates, namely Whatman No. 1, 602 H, 540, 541 and 542, with different particle sizes, particle retention and chemical treatment was then evaluated. As shown in Fig. S2, the highest analytical response was obtained with both Whatman No. 1 and 541. These positive results could be attributed to the highest particle retention of the substrates (11 and 22 µm, respectively). Conversely, Whatman No. 542 showed the lowest analytical response, probably due to its low particle retention (2.7 µm). According to the above results, Whatman No.1 was selected as cellulose substrate for subsequent studies.

The diameter of reservoirs of the three areas of the 3D µPAD, namely donor, reaction and detection areas, can be of utmost importance. Thus, µPADs prepared with combinations of donor and reaction reservoir diameters in the range 4–6 mm and detection reservoir diameters in the range 2–4 mm were tested. As shown in Fig. 5A and B, the µPAD design showed a very relevant effect not only in terms of sensitivity but also in terms of repeatability as a result of the greater or lesser homogeneity of the colored product obtained in the detection zone (Fig. 5C and D). A donor and reaction reservoir diameter of 4 mm and detection reservoir

diameter of 3 mm were selected since they ensured the highest sensitivity and precision.

The effect of sample volume on the analytical response was subsequently studied in the range of 15–60 µL, showing a linear increase of the analytical response from 15 to 30 µL (Fig. S3A). Above this volume, the analytical response reached a plateau or decreased slightly. Thus, a 35 µL sample volume was selected for enhanced sensitivity. Also, the reaction time was evaluated in this work and, as shown in the Fig. S3B, the highest analytical response for both I⁻ and IO₃⁻ was obtained within 1 min, whereas the use of longer reaction times led to a slight decrease on the analytical signal. Therefore, a reaction time of 1 min was selected to ensure high sensitivity and sample throughput.

The amount of reagents present in the different reaction and detection reservoirs was evaluated (Fig. S4). As shown in Fig. S4A, an increase of the amount of starch in the detection area resulted in an increase of the analytical response in the whole evaluated range. Therefore, 100 µg of starch was selected for further studies. The effect of the amount of reagents required to form the triiodide ion in the reaction zones, namely KI (for IO₃⁻ determination), KIO₃ (for I⁻ determination) and citric acid, was then evaluated and the obtained results are provided in Fig. S4B and C. Accordingly, a mass of 125 µg of KI, 160 µg of KIO₃ and 210 µg of citric acid monohydrate was selected to ensure the highest sensitivity.

Finally, the effect of the pH of the aqueous solutions (blanks and standards) on the analytical response was evaluated (Fig. S5). As can be deduced from the Figure, the analytical response was not affected by the pH of the solution over a broad pH range (1−7), whereas a gradual decrease on the response was observed at alkaline pH values for both iodide and iodate (ca. 30–35% decrease at pH 13). This negative effect could be attributed to a partial neutralization of the CA present in the reaction areas of the 3D µPAD, leading to a non-optimal CA amount for
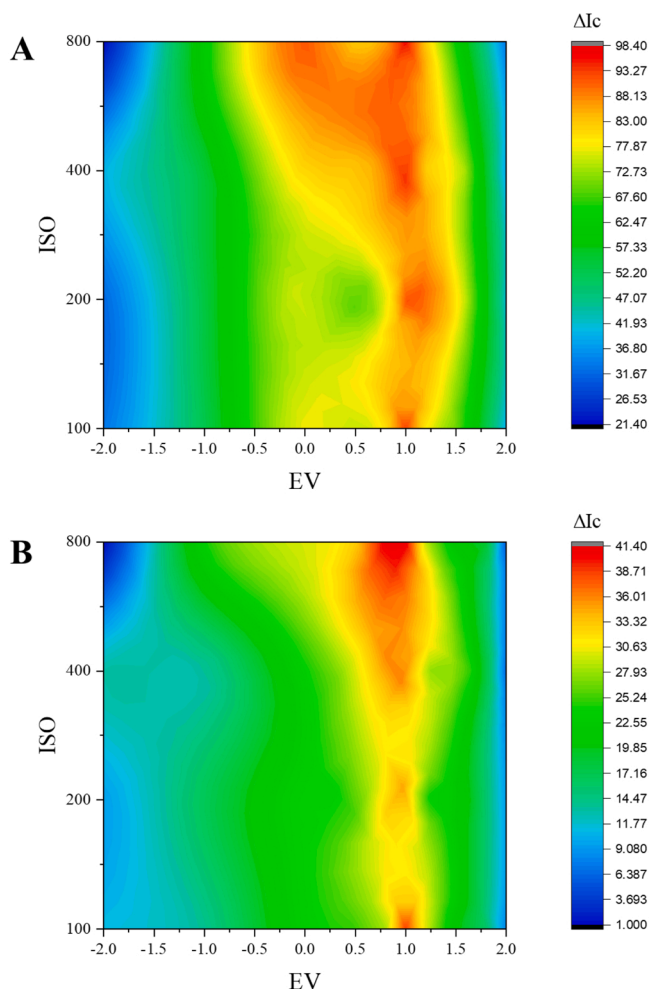
Fig. 4. Effect of EV and ISO on the analytical response for iodide (A) and iodate (B).

the formation of the colored product (Fig. S4C). Thus, pH adjustment of aqueous extracts might be needed for analysis.

3.2. Evaluation of potential interferences

The effect of a number of species present in edible seaweeds and associated food additives that could be extracted and potentially interfere in the determination of iodine species has been assessed. The evaluated species have been considered to interfere when a variation of more than $\pm 10\%$ of the analytical response occurred under optimal conditions (Section 2.6). The assay showed remarkable selectivity, since non-significant effects on the analytical signal were observed when standard solutions of iodide and iodate were analyzed in the presence of 1500 mM H_2PO_4, 900 mM Na^+, 800 mM Mg^{2+}, 625 μM Br^-, 550 mM Cl^-; 500 mM K^+, 50 mM NO_3^-; 25 mM Ca^{2+}, 17 mM HCO_3^-; 4.3 mM NO_2^-, 3 mM SO_4^{2-} and 4.4 μM humic acid.

3.3. Assessment of the stability of the 3D μPAD

The stability of 3D μPADs modified with the required chemicals for iodine speciation (Section 2.6) has been evaluated under four different storage conditions, namely room temperature (both protected (desiccator) and unprotected from humidity), 4 °C (refrigerator) and -20 °C (freezer) for eight consecutive days (Fig. S6). A variation of more than $\pm 10\%$ of the analytical response obtained the same day of fabrication of the μPAD was considered significant. In general terms, the highest stability was achieved by storing the 3D μPADs at -20 °C, whereas PADs

stored at 4 °C or at room temperature in a desiccator showed better stability than stored at room temperature unprotected from humidity. After eight days of storage, the PADs were functional irrespective of the storage conditions, even though with a sensitivity reduction of ca. 45% in the worst case. According to the above results, the 3D μPADs do not need to be prepared the same day of analysis but conveniently fabricated even five days before use without any significant loss of sensitivity when stored at -20 °C.

3.4. Assessment of the methacrylate holder

The performance of the 3D μPAD for the simultaneous determination of iodine species was assessed by using the methacrylate holder developed in this work (Section 2.5) and compared with two alternative strategies reported in the literature to ensure interlayer contact, namely commercial double-clip clamps and staples (Fig. S7) [27,28]. As can be deduced from Fig. 6, a 1.1- to 2.1-fold increase of sensibility was achieved with the reported methacrylate holder in comparison with the use of clamps and staples. In addition, the reported holder enabled the achievement of more precise results (1.7% and 3.3% for I^- and IO_3^-, N = 14) than those obtained with double-clip clamps (5.8% and 5.9% for I^- and IO_3^-, N = 8) and staples (7.9% and 8.0%, for I^- and IO_3^-, N = 8), respectively. The enhanced sensitivity and precision achieved with the methacrylate holder could be attributed to the improved and reproducible interlayer contact, which ensures a larger amount of iodine species reaching the detection areas and leads to the homogeneous formation of the colored product in the detection area.

4. Analytical performance

The analytical characteristics of the proposed method were evaluated under optimal conditions. Non-linear calibration curves were obtained for the determination of both iodine species (Fig. S8A and B), as commonly reported with PADs involving colorimetric detection [37,38]. A rectangular hyperbolic function was used in this work to fit the calibration data, as proposed in the literature [37,38]. A good agreement was obtained when comparing the experimental and estimated concentration values, calculated as $K/((\Delta I_{max}/\Delta I)-1)$, where ΔI is the analytical response, ΔI_{max} is the maximum achievable analytical response, and K is the concentration of each iodine species corresponding to $\Delta I_{max}/2$. The values of ΔI_{max} and K, estimated using the Excel's Solver tool (Microsoft 365), were 148.8 and 514.0 μM for I^- and 133.3 and 28.6 μM for IO_3^-, respectively. The limits of detection (LODs) and quantification (LOQs), calculated according to the 3σ and 10σ criteria, were 9.8 and 32.7 μM for I^- and 0.6 and 1.8 μM for IO_3^-, respectively. Thus, methodological LODs and LOQs were found to be 6.2 and 20.8 μg/g for I^- and 0.4 and 1.1 μg/g for IO_3^-, respectively. The repeatability of the method, expressed as relative standard deviation (RSD) and evaluated from fourteen consecutive measurements at 500 μM for I^- and 25 μM for IO_3^-, was 1.7% and 3.3%, respectively.

A comparison of the proposed 3D μPAD with instrumental methods reported in the literature for determination of I^- and IO_3^- in seaweed samples is shown in Table 1. The proposed assay shows LODs beyond those of the instrumental methods considered in Table 1, even though sufficient for monitoring iodine species in algal products that could lead to dangerously excessive iodine intakes. The analysis time of the proposed method is lower than that of HPLC-ICP-MS methods [10,11,39], and comparable to the ones reported for a sequential injection standard addition method [13]. Besides, the sample volume used (35 μL) is similar to or lower than that reported in alternative methods [10–13,39].

Finally, the developed 3D μPAD was applied to the determination of I^- and IO_3^- in extracts of edible seaweeds and related food additives purchased at a local market (Table 2). Particularly, the study included three types of edible seaweed, namely Kombu (*Laminaria ochroleuca*), Sea Lettuce (*Ulva rigida*) and Nori (*Porphyra umbilicalis*), and agar-agar, a combination of polysaccharides produced by a number of species of red
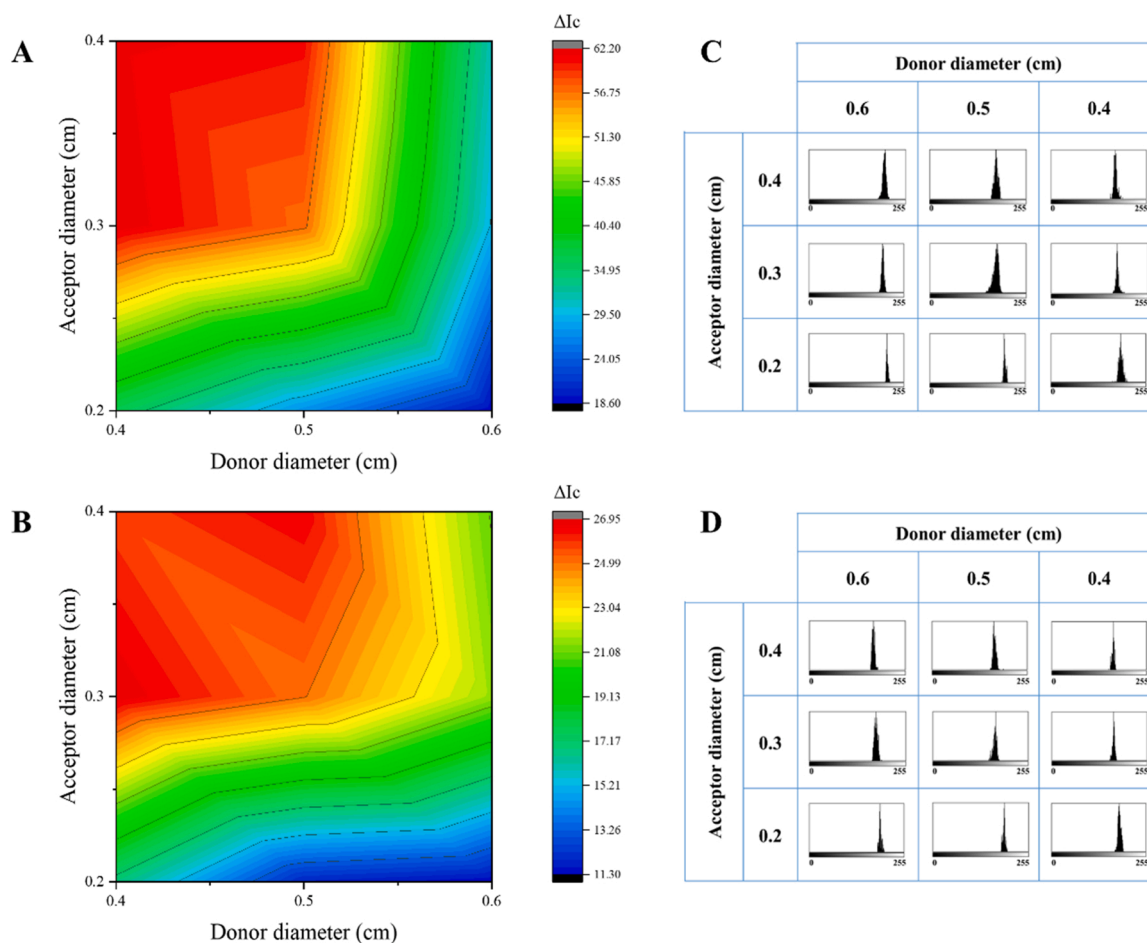
Fig. 5. Effect of the diameter of donor and acceptor reservoirs of µPADs on the analytical response for iodide (A) and iodate (B). Histograms of the detection areas of µPADs obtained with the evaluated dimensions for the determination of iodide (C) and iodate (D).
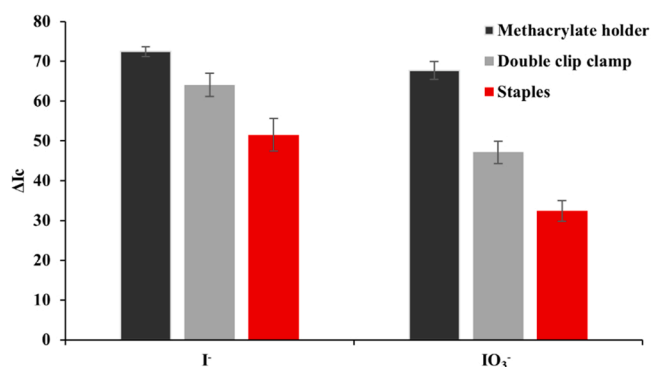

Fig. 6. Analytical responses obtained with different holders for I^- and IO_3^- determination.

macroalgae (Rodophyceae) and commonly used as food additive (E 406). The pH of aqueous and acidic extracts of seaweed and related food additives analyzed in this work was about 2 and 6, so additional pH adjustments of extracts were not required for the analysis (*Section 3.1*). As shown in Table 2, the concentrations of iodine species depended to a high extent on the type of seaweed studied, being especially high in Kombu seaweed. Both I^- and IO_3^- were found in the water-soluble fraction and acidic extracts of two seaweed samples, namely Kombu and Nori, the obtained results being in good agreement with the content ranges reported in the literature [40,41]. In addition, recovery studies were performed at two concentration levels, with recoveries in the range

of 90–109% and 90–107% for I^- and IO_3^-, respectively. Thus, the colorimetric assay was not significantly affected by matrix effects.

5. Conclusions

This work reports the development of a straightforward, inexpensive and environmentally friendly colorimetric assay for determination of I^- and IO_3^- in seaweed extract fractions using 3D µPADs. The proposed approach, based on the formation of the colored I_3^--starch complex on the detection area of the µPAD, represents an advantageous alternative to instrumental methods for the determination of inorganic iodine species in algae and algae-related products. Furthermore, the methacrylate holder designed in this work, suitable with virtually any design of 3D µPAD, was found advantageous over other alternatives reported in the literature. The reported holder demonstrated improved interlayer contact in 3D µPADs, resulting in enhanced sensitivity and precision while enabling real-time monitoring in a straightforward and expeditious way.

CRediT authorship contribution statement

Lorena Placer: Investigation, Methodology, Writing – review & editing. **Isela Lavilla**: Data curation, Writing – review & editing. **Francisco Pena-Pereira**: Conceptualization, Investigation, Supervision, Writing – original draft. **Carlos Bendicho**: Conceptualization, Supervision, Writing – review & editing, Funding acquisition.

Table 1

Comparison of methods for I^- and IO_3^- determination in seaweeds.

Analytical Method	Iodine species	LOD (μM)	Repeatability (%, RSD)	Sample volume (μL)	Analysis time (min)	Ref.
IC-ICP-MS	I^-	0.0009	1.0%	20	10	[39]
	IO_3^-	0.0011	1.2%			
Reverse phase-HPLC-ICP-MS	I^-	0.0005	4%	20	5	[10]
	IO_3^-	0.0003				
Anion-exchange-HPLC-ICP-MS	I^-	0.25	6%	25	20	[11]
	IO_3^-	0.20				
CE-UV	I^-	0.41	3%	2	7	[12]
	IO_3^-	0.23				
SI-ISE	I^-	0.14	4.2%	164	1.3	[13]
SI-UV–vis	IO_3^-	0.02	4.1%	900	3.6	[13]
3D μPAD-smartphone-based colorimetric detection	I^-	9.8	1.7%	35	1	This work
	IO_3^-	0.6	3.3%			

CE-UV, capillary electrophoresis-UV detection; IC, Ion chromatography; RP-HPLC, reverse phase high performance liquid chromatography; SI-ISE, sequential injection-ion selective electrode.

Table 2

Analytical results obtained for the determination of I^- and IO_3^- in aqueous and acidic extracts of seaweed samples.

Seaweed samples	Added I^- concentration (μg/g)	Found I^- concentration (μg/g)	Recovery (%)	Added IO_3^- concentration (μg/g)	Found IO_3^- concentration (μg/g)	Recovery (%)
Water-soluble extracts						
Kombu	–	2399 ± 192[a]		–	136 ± 12	
	635	3064 ± 184	101 ± 6	87.5	232 ± 21	104 ± 9
	1270	3999 ± 240	109 ± 6	175	320 ± 13	103 ± 4
Nori	–	92 ± 6		–	7.2 ± 0.4	
	63.5	157 ± 9	101 ± 6	8.75	16.9 ± 0.8	107 ± 5
	127	199 ± 16	91 ± 8	17.5	25.7 ± 1.0	105 ± 4
Sea lettuce	–	<LOD		–	<LOD	
	63.5	67 ± 7	106 ± 10	8.75	8.8 ± 0.8	101 ± 9
	127	138 ± 10	109 ± 7	17.5	17.1 ± 0.7	98 ± 4
Agar-agar	–	<LOD		–	<LOD	
	63.5	63 ± 3	99 ± 5	8.75	8.6 ± 0.9	98 ± 10
	127	125 ± 6	98 ± 5	17.5	18.0 ± 1.3	103 ± 7
Acidic extracts						
Kombu	–	2433 ± 219[a]		–	302 ± 27	
	635	3160 ± 221	103 ± 7	87.5	370 ± 30	95 ± 8
	1270	3777 ± 340	102 ± 9	175	458 ± 41	96 ± 9
Nori	–	93 ± 5		–	14 ± 1	
	63.5	150 ± 11	96 ± 7	8.75	23 ± 2	100 ± 7
	127	216 ± 19	98 ± 9	17.5	28 ± 1	90 ± 4
Sea lettuce	–	<LOD		–	<LOD	
	63.5	68 ± 1	107 ± 2	8.75	8.5 ± 0.5	97 ± 6
	127	136 ± 4	107 ± 3	17.5	17.3 ± 0.5	99 ± 3
Agar-agar	–	<LOD		–	<LOD	
	63.5	68 ± 5	107 ± 8	8.75	8.1 ± 0.4	93 ± 5
	127	119 ± 7	94 ± 6	17.5	19.1 ± 1.9	109 ± 10

[a] After 10-fold dilution

Declaration of Competing Interest

The authors declare that they have no known competing financial interests or personal relationships that could have appeared to influence the work reported in this paper.

Data availability

Data will be made available on request.

Appendix A. Supplementary material

Supplementary data associated with this article can be found in the online version at doi:10.1016/j.snb.2022.133109.

References

[1] M.R. Domínguez-González, G.M. Chiocchetti, P. Herbello-Hermelo, D. Vélez, V. Devesa, P. Bermejo-Barrera, Evaluation of iodine bioavailability in seaweed using in vitro methods, J. Agric. Food Chem. 65 (2017) 8435–8442, https://doi.org/10.1021/acs.jafc.7b02151.

[2] M.J. Blikra, S. Henjum, I. Aakre, Iodine from brown algae in human nutrition, with an emphasis on bioaccessibility, bioavailability, chemistry, and effects of processing: a systematic review, Compr. Rev. Food Sci. Food Saf. 21 (2022) 1517–1536, https://doi.org/10.1111/1541-4337.12918.

[3] K. Miyai, T. Tokushige, M. Kondo, Suppression of thyroid function during ingestion of seaweed "Kombu" (*Laminaria japonica*) in normal Japanese adults, Endocr. J. 55 (2008) 1103–1108, https://doi.org/10.1507/endocrj.K08E-125.

[4] A. Moreda-Pineiro, V. Romarís-Hortas, P. Bermejo-Barrera, A review on iodine speciation for environmental, biological and nutrition fields, J. Anal. At. Spectrom. 26 (2011) 2107–2152, https://doi.org/10.1039/c0ja00272k.

[5] M. Andersson, B. de Benoist, I. Darnton-Hill, F. Delange, Iodine Deficiency in Europe: A Continuing Public Health Problem, World Health Organization, Geneva, Switzerland, 2007.

[6] J. Farebrother, M.B. Zimmermann, M. Andersson, Excess iodine intake: sources, assessment, and effects on thyroid function, Ann. N. Y. Acad. Sci. 1446 (2019) 44–65, https://doi.org/10.1111/nyas.14041.

[7] Institute of Medicine Panel on Micronutrients, Dietary reference intakes for vitamin A, vitamin K, arsenic, boron, chromium, copper, iodine, iron, manganese, molybdenum, nickel, silicon, vanadium, and zinc, National Academies Press (US), Washington (DC), 2001.

[8] European Union, Commission recommendation (EU) 2018/464 of 19 March 2018 on the monitoring of metals and iodine in seaweed, halophytes and products based on seaweed, Off. J. Eur. Union. 78 (2018) (2018) 16–18.

[9] X. Hou, C. Chai, Q. Qian, X. Yan, X. Fan, Determination of chemical species of iodine in some seaweeds (I), Sci. Total Environ. 204 (1997) 215–221, https://doi.org/10.1016/S0048-9697(97)00182-4.

[10] X. Han, L. Cao, H. Cheng, J. Liu, Z. Xu, Determination of iodine species in seaweed and seawater samples using ion-pair reversed phase high performance liquid chromatography coupled with inductively coupled plasma mass spectrometry, Anal. Methods 4 (2012) 3471–3477, https://doi.org/10.1039/c2ay25871d.

[11] V. Romarís-Hortas, P. Bermejo-Barrera, A. Moreda-Piñeiro, Development of anion-exchange/reversed-phase high performance liquid chromatography-inductively coupled plasma-mass spectrometry methods for the speciation of bio-available iodine and bromine from edible seaweed, J. Chromatogr. A 1236 (2012) 164–176, https://doi.org/10.1016/j.chroma.2012.03.019.

[12] J. Sun, D. Wang, H. Cheng, J. Liu, Y. Wang, Z. Xu, Use of ion-pairing reagent for improving iodine speciation analysis in seaweed by pressure-driven capillary electrophoresis and ultraviolet detection, J. Chromatogr. A 1379 (2015) 112–117, https://doi.org/10.1016/j.chroma.2014.12.056.

[13] I.C. Santos, R.B.R. Mesquita, A.A. Bordalo, A.O.S.S. Rangel, Iodine speciation in coastal and inland bathing waters and seaweeds extracts using a sequential injection standard addition flow-batch method, Talanta 133 (2015) 7–14, https://doi.org/10.1016/j.talanta.2014.01.025.

[14] U. Nitschke, D.B. Stengel, A new HPLC method for the detection of iodine applied to natural samples of edible seaweeds and commercial seaweed food products, Food Chem. 172 (2015) 326–334, https://doi.org/10.1016/j.foodchem.2014.09.030.

[15] J.L.A. Miranda, R.B.R. Mesquita, E. Palacio, J.M. Estela, V. Cerdà, A.O.S.S. Rangel, Chip-based spectrofluorimetric determination of iodine in a multi-syringe flow platform with and without in-line digestion—application to salt, pharmaceuticals, and algae samples, Molecules 27 (2022) 1325, https://doi.org/10.3390/molecules27041325.

[16] K. Grudpan, S.D. Kolev, S. Lapanantnopakhun, I.D. Mckelvie, W. Wongwilai, Applications of everyday IT and communications devices in modern analytical chemistry: a review, Talanta 136 (2015) 84–94, https://doi.org/10.1016/j.talanta.2014.12.042.

[17] A.W. Martinez, S.T. Phillips, G.M. Whitesides, Three-dimensional microfluidic devices fabricated in layered paper and tape, Proc. Natl. Acad. Sci. USA 105 (2008) 19606–19611, https://doi.org/10.1073/pnas.0810903105.

[18] F. Arduini, S. Cinti, V. Caratelli, L. Amendola, G. Palleschi, D. Moscone, Origami multiple paper-based electrochemical biosensors for pesticide detection, Biosens. Bioelectron. 126 (2019) 346–354, https://doi.org/10.1016/j.bios.2018.10.014.

[19] E. Noviana, D.B. Carrão, R. Pratiwi, C.S. Henry, Emerging applications of paper-based analytical devices for drug analysis: a review, Anal. Chim. Acta 1116 (2020) 70–90, https://doi.org/10.1016/j.aca.2020.03.013.

[20] B. Li, Z. Zhang, J. Qi, N. Zhou, S. Qin, J. Choo, L. Chen, Quantum dot-based molecularly imprinted polymers on three-dimensional origami paper microfluidic chip for fluorescence detection of phycocyanin, ACS Sens. 2 (2017) 243–250, https://doi.org/10.1021/acssensors.6b00664.

[21] C. Ma, W. Li, Q. Kong, H. Yang, Z. Bian, X. Song, J. Yu, M. Yan, 3D origami electrochemical immunodevice for sensitive point-of-care testing based on dual-signal amplification strategy, Biosens. Bioelectron. 63 (2015) 7–13, https://doi.org/10.1016/j.bios.2014.07.014.

[22] Y. Zhu, X. Tong, Q. Wei, G. Cai, Y. Cao, C. Tong, S. Shi, F. Wang, 3D origami paper-based ratiometric fluorescent microfluidic device for visual point-of-care detection of alkaline phosphatase and butyrylcholinesterase, Biosens. Bioelectron. 196 (2022), 113691, https://doi.org/10.1016/j.bios.2021.113691.

[23] J. Lee, Y.K. Yoo, D. Lee, C. Kim, K.H. Kim, S. Lee, S. Kwak, J.Y. Kang, H. Kim, D.S. Yoon, D. Hur, J.H. Lee, Origami paper-based sample preconcentration using sequentially driven ion concentration polarization, Lab Chip 21 (2021) 867–874, https://doi.org/10.1039/d0lc01032d.

[24] J.S. Ng, M. Hashimoto, 3D-PAD: paper-based analytical devices with integrated three-dimensional features, Biosensors 11 (2021) 1–13, https://doi.org/10.3390/bios11030084.

[25] J. Qi, B. Li, X. Wang, Z. Zhang, Z. Wang, J. Han, L. Chen, Three-dimensional paper-based microfluidic chip device for multiplexed fluorescence detection of Cu^{2+} and Hg^{2+} ions based on ion imprinting technology, Sens. Actuators B Chem. 251 (2017) 224–233, https://doi.org/10.1016/j.snb.2017.05.052.

[26] J. Sitanurak, N. Wangdi, T. Sonsa-ard, S. Teerasong, T. Amornsakchai, D. Nacapricha, Simple and green method for direct quantification of hypochlorite in household bleach with membraneless gas-separation microfluidic paper-based analytical device, Talanta 187 (2018) 91–98, https://doi.org/10.1016/j.talanta.2018.04.077.

[27] L. Xiao, X. Liu, R. Zhong, K. Zhang, X. Zhang, X. Zhou, B. Lin, Y. Du, A rapid, straightforward, and print house compatible mass fabrication method for integrating 3D paper-based microfluidics, Electrophoresis 34 (2013) 3003–3007, https://doi.org/10.1002/elps.201300198.

[28] H. Liu, R.M. Crooks, Three-dimensional paper microfluidic devices assembled using the principles of origami, J. Am. Chem. Soc. 133 (2011) 17564–17566, https://doi.org/10.1021/ja2071779.

[29] C.A. Schneider, W.S. Rasband, K.W. Eliceiri, NIH image to ImageJ: 25 years of image analysis, Nat. Methods 9 (2012) 671–675, https://doi.org/10.1038/nmeth.2089.

[30] R.E. Rundle, J.F. Foster, B.R. R, On the nature of the starch-iodine complex, J. Am. Chem. Soc. 66 (1944) 2116–2120, https://doi.org/10.2139/ssrn.1836494.

[31] N.M.K. Ng Ying Kin, W. Yaphe, Properties of agar: parameters affecting gel-formation and the agarose-iodide reaction, Carbohydr. Res. 25 (1972) 379–385, https://doi.org/10.1016/S0008-6215(00)81648-1.

[32] D.B. Gazda, R.J. Lipert, J.S. Fritz, M.D. Porter, Investigation of the iodine-poly (vinylpyrrolidone) interaction employed in the determination of biocidal iodine by colorimetric solid-phase extraction, Anal. Chim. Acta 510 (2004) 241–247, https://doi.org/10.1016/j.aca.2004.01.010.

[33] M.P. Arena, M.D. Porter, J.S. Fritz, Rapid, specific determination of iodine and iodide by combined solid-phase extraction/diffuse reflectance spectroscopy, Anal. Chem. 74 (2002) 185–190, https://doi.org/10.1021/ac0109366.

[34] P.R. Bhagat, A.K. Pandey, R. Acharya, V. Natarajan, N.S. Rajurkar, A.V.R. Reddy, Molecular iodine selective membrane for iodate determination in salt samples: chemical amplification and preconcentration, Anal. Bioanal. Chem. 391 (2008) 1081–1089, https://doi.org/10.1007/s00216-008-2057-1.

[35] G. Li, C. Yan, B. Cao, J. Jiang, W. Zhao, J. Wang, T. Mu, Highly efficient I_2 capture by simple and low-cost deep eutectic solvents, Green Chem. 18 (2016) 2522–2527, https://doi.org/10.1039/c5gc02691a.

[36] X. Du, H. An, Z. Liu, H. Yang, L. Wei, Probing starch-iodine interaction by atomic force microscopy, Scanning 36 (2014) 394–400, https://doi.org/10.1002/sca.21131.

[37] C.A. Chaplan, H.T. Mitchell, A.W. Martinez, Paper-based standard addition assays, Anal. Methods 6 (2014) 1296–1300, https://doi.org/10.1039/C4AY00205A.

[38] F. Pena-Pereira, I. Lavilla, C. Bendicho, Paper-based analytical device for instrumental-free detection of thiocyanate in saliva as a biomarker of tobacco smoke exposure, Talanta 147 (2016) 390–396, https://doi.org/10.1016/j.talanta.2015.10.013.

[39] M. Shah, R.G. Wuilloud, S.S. Kannamkumarath, J.A. Caruso, Iodine speciation studies in commercially available seaweed by coupling different chromatographic techniques with UV and ICP-MS detection, J. Anal. At. Spectrom. 20 (2005) 176–182, https://doi.org/10.1039/b415756g.

[40] T.S. Yeh, N.H. Hung, T.C. Lin, Analysis of iodine content in seaweed by GC-ECD and estimation of iodine intake, J. Food Drug Anal. 22 (2014) 189–196, https://doi.org/10.1016/j.jfda.2014.01.014.

[41] V. Romarís-Hortas, A. Moreda-Piñeiro, P. Bermejo-Barrera, Microwave assisted extraction of iodine and bromine from edible seaweed for inductively coupled plasma-mass spectrometry determination, Talanta 79 (2009) 947–952, https://doi.org/10.1016/j.talanta.2009.05.036.

Lorena Placer is a Ph.D. student at the Department of Food and Analytical Chemistry of the Vigo University. She focuses on the development of optical sensing approaches for environmental assessment.

Isela Lavilla obtained her Ph.D. at the University of Zaragoza (December 1993). She became Associate Professor of Analytical Chemistry in the University of Vigo in 2002. Her research interests include development of new sample preparation methods for trace element analysis and speciation. Her Hirsch-index is 44 (Scopus).

Francisco Pena-Pereira received his Ph.D. (2009) in Chemistry from the University of Vigo (Spain). He then joined the Center for Environmental and Marine Studies (CESAM), University of Aveiro (Portugal) & Gdańsk University of Technology (Poland) as a post-doctoral fellow (2011–2015). At present, he focuses on the implementation of nano-materials in miniaturized systems for analyte sensing at the University of Vigo (Spain). His Hirsch-index is 33 (Scopus).

Carlos Bendicho received B.S., M.S. and Ph.D. degrees in Chemistry from the University of Zaragoza (Spain), in 1983, 1984 and 1987, respectively. In 1988–1990, he was working as a postdoctoral fellow in the Technical University of Delft (The Netherlands). Currently, he is full professor of Analytical Chemistry at the Vigo University. His research focuses on analytical nanoscience and nanotechnology, optical sensors, microfluidics, paper-based analytical devices and point-of-care testing for trace element analysis and speciation in environmental and food samples. He is author of about 200 scientific publications and has supervised 15 Ph.D. and 40 MSc. students. His Hirsch-index is 47 (Scopus).